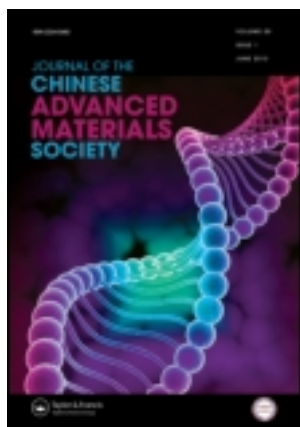


This article was downloaded by: [University of California Santa Cruz]

On: 26 September 2013, At: 08:43

Publisher: Taylor & Francis

Informa Ltd Registered in England and Wales Registered Number: 1072954 Registered office: Mortimer House, 37-41 Mortimer Street, London W1T 3JH, UK



Journal of the Chinese Advanced Materials Society

Publication details, including instructions for authors and subscription information:

<http://www.tandfonline.com/loi/tadm20>

TiO₂ nanotubes/ZnO/CdS ternary nanocomposites: preparation, characterization and photocatalysis

Chan Lin^{a b}, Yang Song^b, Lixin Cao^c & Shaowei Chen^b

^a College of Chemistry and Chemical Engineering, Ocean University of China, Qingdao, China

^b Department of Chemistry and Biochemistry, University of California, Santa Cruz, CA, USA

^c Institute of Materials Science and Engineering, Ocean University of China, Qingdao, China

To cite this article: Chan Lin, Yang Song, Lixin Cao & Shaowei Chen (2013) TiO₂ nanotubes/ZnO/CdS ternary nanocomposites: preparation, characterization and photocatalysis, Journal of the Chinese Advanced Materials Society, 1:3, 188-199, DOI: [10.1080/22243682.2013.832499](https://doi.org/10.1080/22243682.2013.832499)

To link to this article: <http://dx.doi.org/10.1080/22243682.2013.832499>

PLEASE SCROLL DOWN FOR ARTICLE

Taylor & Francis makes every effort to ensure the accuracy of all the information (the "Content") contained in the publications on our platform. However, Taylor & Francis, our agents, and our licensors make no representations or warranties whatsoever as to the accuracy, completeness, or suitability for any purpose of the Content. Any opinions and views expressed in this publication are the opinions and views of the authors, and are not the views of or endorsed by Taylor & Francis. The accuracy of the Content should not be relied upon and should be independently verified with primary sources of information. Taylor and Francis shall not be liable for any losses, actions, claims, proceedings, demands, costs, expenses, damages, and other liabilities whatsoever or howsoever caused arising directly or indirectly in connection with, in relation to or arising out of the use of the Content.

This article may be used for research, teaching, and private study purposes. Any substantial or systematic reproduction, redistribution, reselling, loan, sub-licensing, systematic supply, or distribution in any form to anyone is expressly forbidden. Terms &

Conditions of access and use can be found at <http://www.tandfonline.com/page/terms-and-conditions>

TiO₂ nanotubes/ZnO/CdS ternary nanocomposites: preparation, characterization and photocatalysis

Chan Lin^{a,b}, Yang Song^b, Lixin Cao^{c*} and Shaowei Chen^{b*}

^aCollege of Chemistry and Chemical Engineering, Ocean University of China, Qingdao, China;

^bDepartment of Chemistry and Biochemistry, University of California, Santa Cruz, CA, USA;

^cInstitute of Materials Science and Engineering, Ocean University of China, Qingdao, China

(Received 21 June 2013; revised 21 July 2013; accepted 30 July 2013)

TiO₂ nanotube arrays were prepared by electroanodization of titanium metal foils, and then modified with two semiconductor thin films. First, a ZnO layer was deposited onto the TiO₂ surface by sequential chemical bath deposition of a zinc salt complex followed by a thermal annealing process. A CdS thin film was then formed on the TiO₂/ZnO surface by layer-by-layer deposition of Cd(NO₃)₂ and Na₂S, leading to the production of ternary TiO₂/ZnO/CdS nanocomposites. The structures of the resulting nanocomposites were characterized by using a variety of experimental tools including field-emission scanning electron microscopy, X-ray diffraction, X-ray photoelectron and ultraviolet-visible (UV-vis) diffuse reflectance spectroscopy. Importantly, the resulting nanocomposites exhibited markedly enhanced photocatalytic activity, as highlighted by the photodegradation of alizarin red S under UV light, in comparison to the unmodified TiO₂ nanotubes or the nanotubes modified only with ZnO or CdS. This was accounted for by the formation of a cascade of electronic energy structures within the ternary hybrids that facilitated charge separation and reduced the recombination of the photoinduced electron-hole pairs.

Keywords: TiO₂ nanotube; TiO₂/ZnO/CdS ternary hybrid; photocatalysis; alizarin red S

1. Introduction

In recent years, effective removal of organic dyes has attracted increasing interest because of the long-term environmental toxicity and short-term hazards of organic dyes to public health.[1,2] Various metal oxides have been extensively examined as potential photocatalysts for the degradation of organic dyes.[3–6] Among these, TiO₂ has been widely used because of its low cost, chemical inertness and good photostability.[7–9] However, with a large band gap (3.0–3.2 eV) TiO₂ can absorb only ultraviolet (UV) light, which accounts only for 4–5% in the solar spectrum. To increase light utilization efficiency, a variety of approaches have been developed to engineer the oxide structures and properties, such as doping with metal and nonmetal elements, combination with other semiconductor materials, sensitization by organometallic dye molecules, etc.[10–17] In these, the formation of a stepwise band gap structure in the composites with other semiconductor materials has been found to lead to a superior photocatalytic performance because the resulting catalysts not only extend light absorption to the visible region, but also exhibit a reduced recombination rate of photogenerated electron-hole pairs.[18] In previous studies, extensive investigations have been concentrated on the design and synthesis of binary semiconductor metal oxides such as TiO₂/ZnO and TiO₂/CdS nanocomposite materials to

*Corresponding authors. Email: caolixin@ouc.edu.cn; shaowei@ucsc.edu

improve the photocatalytic quantum efficiency in water purification and degradation of organic pollutants.[19,20] The improvement is largely attributed to the formation of a potential gradient at the interface. To further improve the photocatalytic performance, ternary hybrid systems have also received particular attention. For instance, Kim et al. [18] reported the synthesis of CdS/TiO₂/WO₃ ternary hybrid systems as new photoactive composites and found that the ternary hybrid exhibited much higher photocatalytic activity than that of CdS alone or binary hybrids. In another study, Lin et al. [21] prepared CdS nanoparticles/ZnO shell/TiO₂ nanotube (NT) arrays for water splitting and found that the conversion efficiency increased from 0.39% to 1.30%. Furthermore, Chen et al. [22] described a new method to form a ZnO energy barrier layer between TiO₂ NTs and CdS quantum dots, which exhibited improved efficiency of the quantum dots-sensitized solar cells. These earlier successes are the primary motivation of the present study.

In this study, a ternary functional semiconductor composite TiO₂/ZnO/CdS was prepared by sequential deposition of ZnO and CdS nanostructures onto TiO₂ NT array surfaces. Experimentally, TiO₂ NTs were first synthesized by electrochemical anodization of titanium metal foils, which were then coated with a thin layer of ZnO by thermal treatments of Zn(II) complexes adsorbed onto the TiO₂ surfaces. A third layer of CdS nanostructures was formed by a chemical bath deposition method where Cd(II) and sulfide precursors were both deposited onto the NT surfaces. The resulting ternary hybrids exhibited apparent photocatalytic activity, as highlighted by the degradation under UV photoirradiation of alizarin red S (ARS), an anthraquinone dye with high toxicity and high chemical oxygen demand. Such a performance was markedly better than that of the unmodified TiO₂ NTs or the binary hybrids of TiO₂/CdS or TiO₂/ZnO. This was accounted for by the formation of a cascade of energy structures within the ternary hybrids that facilitated charge separation and impeded charge recombination at the interface upon UV photoirradiation.

2. Experimental section

2.1. TiO₂ NTs

Titanium (Ti) foils (250 μm in thickness, 99.5% purity) were purchased from Alfa Aesar. The preparation of TiO₂ NTs has been detailed in our previous work.[23,24] Briefly, small Ti pieces of 10 mm × 15 mm were cut from a large Ti foil and ultrasonically cleaned in acetone and anhydrous ethanol for 20 min and 10 min, respectively, washed with deionized water, and finally dried in a nitrogen stream. TiO₂ NTs were prepared by an electrochemical anodization procedure in a conventional two-electrode configuration under magnetic stirring. The titanium foils served as the anode and a graphite sheet as the cathode. The electrolyte was a mixture of glycerol and water (at a volume ratio of 4:1) containing 0.5 wt% NH₄F. All experiments were carried out at a constant potential of 25 V at 25 °C for 10 h. After anodization, the samples were rinsed with deionized water and then kept in a vacuum oven at 100 °C for 12 h.

2.2. TiO₂-based nanocomposites

TiO₂/ZnO binary nanocomposites were prepared by a layer-by-layer deposition method. [25] In a typical reaction, the TiO₂ NTs prepared above were first immersed in an ammonia solution of 0.01 M ZnCl₂ for 30 s, then in distilled water at 95 °C for 30 s. The cycle was repeated for several times, and the obtained samples were dried in air and then

underwent thermal annealing at 450 °C for 180 s, leading to the formation of a thin layer of ZnO on the TiO₂ surface.

The preparation of TiO₂/CdS binary hybrids was carried out by a sequential chemical bath deposition method,[19] where the NTs were immersed sequentially into 0.1 M Cd(NO₃)₂, nanopure water, 0.1 M Na₂S and nanopure water each for 1 min. The cycle was repeated to produce a thin layer of CdS nanostructures on the TiO₂ NT surfaces. The resulting hybrid nanostructures were then rinsed with water and dried in a nitrogen stream.

The TiO₂/ZnO/CdS ternary hybrids were prepared in a similar fashion except that the TiO₂/ZnO binary nanocomposites prepared above were used as the starting materials for the deposition of CdS thin films.

2.3. Characterization

The morphological details of the hybrid materials obtained above were examined by using a field-emission scanning electron microscope (FESEM, Hitachi S-4800). The crystalline properties were analyzed by X-ray diffraction (XRD, BRUKER D8 ADVANCE) with Cu-K α radiation within the 2 θ range of 20°–70° at a scan speed of 5° per min. Optical absorption spectra were acquired by using a diffuse reflectance UV and visible spectrophotometer (Shimadzu UV-2550, Japan). X-ray photoelectron spectra (XPS) were recorded with a PHI 5400 XPS instrument equipped with an Al-K α source operated at 350 W and at 10⁻⁹ torr.

2.4. Photocatalysis

The ARS stock solution was prepared at a concentration of 40 mg L⁻¹ in water with the pH adjusted by NaOH to 9. At the beginning of the reaction, 10 mL of the ARS solution was added to a 25-mL quartz beaker. A calculated amount of the photocatalysts was added into the solution. The distance between the quartz beaker and the UV lamp (385 nm, 300 W) was 10 cm. Prior to exposure to the UV light source, the catalysts were soaked in the ARS solution for at least 30 min in the dark to establish an adsorption/desorption equilibrium. The solution was subject to vigorous stirring during the entire process. At different time intervals after the exposure of the solution to the UV lamp, an aliquot of the solution was removed to record the corresponding optical absorption spectra with a Shimadzu UV-2550 UV-vis spectrophotometer.

3. Results and discussion

The morphological details of the TiO₂ NTs were first examined by SEM measurements. Figure 1 (a) shows a representative SEM NT image of TiO₂ NTs that were prepared by electroanodization of Ti foils at 25 V and 25 °C for 10 h in the mixed solution of glycerol and water. It can be seen that the inner diameter of the NTs is approximately 90 nm with the wall thickness of about 16 nm, corresponding to a specific surface area of at least 59 m² g⁻¹. After seven cycles of deposition of an ammonia solution of ZnCl₂, thermal treatment led to the formation of a ZnO network on the TiO₂ surfaces with a thickness of about 15 nm, as revealed in panel (b). The formation of CdS nanostructures on TiO₂ NTs can also be seen in panel (c), where clusters of CdS nanoparticles (ca. 10 nm in diameter) were formed, in particular, around the opening of the TiO₂ NTs. More extensive

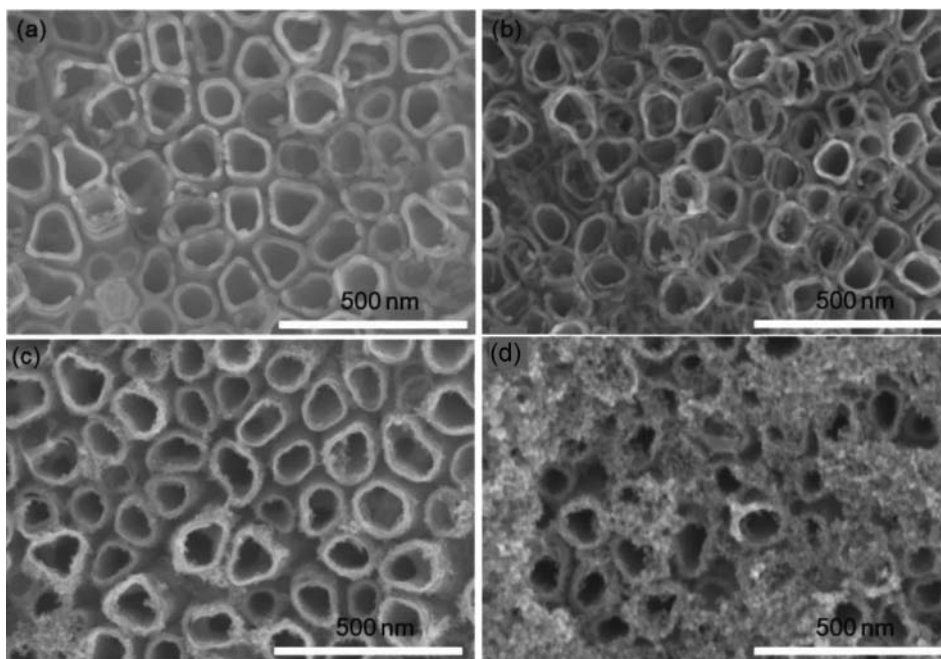


Figure 1. Representative SEM micrographs of (a) TiO_2 nanotubes, (b) TiO_2/ZnO , (c) TiO_2/CdS and (d) $\text{TiO}_2/\text{ZnO}/\text{CdS}$ nanocomposites. Scale bars are all 500 nm.

deposition of CdS nanoparticles (of similar size) can be seen in panel (d) for the $\text{TiO}_2/\text{ZnO}/\text{CdS}$ ternary hybrids.

The crystalline structures of the resulting nanocomposites were further examined by XRD measurements. Figure 2 shows the XRD patterns of the as-prepared TiO_2 NTs and the corresponding hybrids with ZnO and CdS. It can be seen that after thermal annealing at 450°C , the electrochemically prepared TiO_2 NTs (red curve) exhibited well-defined diffraction peaks at 25.4° , 37.8° and 48.0° , which may be assigned to the (101), (004) and (200) crystalline planes of anatase TiO_2 , respectively (additional diffraction features are ascribed to the titanium metal foils that supported the TiO_2 NTs, as depicted in the black curve of the as-prepared TiO_2 NTs). Furthermore, the average size (τ) of the crystalline domains of the TiO_2 NTs can be estimated by the Debye–Scherrer equation,[24] $\tau = K\lambda/\beta \cos \theta$, where K is a dimensionless shape factor with a value of ~ 0.9 , λ is the X-ray wavelength (1.54059 Å for Cu– $K\alpha$) and β is the full width at half maximum of a selected diffraction peak. Therefore, based on the width of the (101) diffraction peak, the average size of the crystalline domains of the TiO_2 NTs was estimated to be 22.92 nm.

For the TiO_2/CdS binary hybrids (green curve), in addition to the TiO_2 (and Ti) diffraction features, a new set of diffraction peaks appeared at 26.5° , 43.9° and 52.1° , which may be assigned to the (111), (220) and (311) crystalline planes of cubic-phase CdS, respectively.[26] For the TiO_2/ZnO binary hybrids (blue curve), several broad peaks can be identified at 31.7° , 34.4° and 36.2° . These are consistent with the (100), (002) and (101) diffraction planes of hexagonal ZnO.[27] The diffraction features of TiO_2 , ZnO and CdS can all be seen in the ternary composites of $\text{TiO}_2/\text{ZnO}/\text{CdS}$ (light blue curve), indicating the successful formation of ternary hybrids.

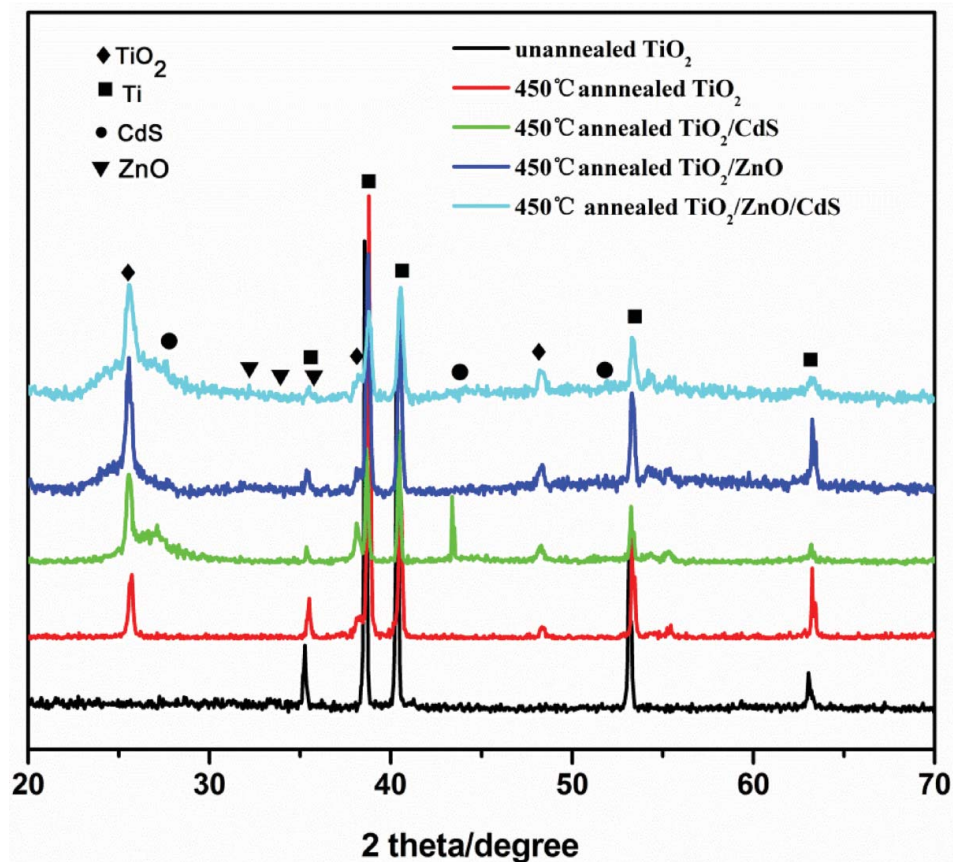


Figure 2. XRD patterns of as-prepared (black curve) and thermally heated (red curve) TiO_2 nanotubes, TiO_2/CdS (green curve), TiO_2/ZnO (blue curve) and $\text{TiO}_2/\text{ZnO}/\text{CdS}$ (light blue curve) nanocomposites.

The compositions of the ternary composites were then evaluated by XPS measurements. Figure 3 (a) depicts the XPS survey spectrum of the $\text{TiO}_2/\text{ZnO}/\text{CdS}$ nanocomposites, where the elements of Ti, Zn, Cd, S and O can all be clearly identified. High-resolution scans showed that Ti $2p$ electrons exhibited a pair of peaks centered at 460.6 eV and 466.3 eV, consistent with those of Ti(IV) in TiO_2 , [28] as depicted in panel (b). Similarly, Zn $2p$ electrons can be found at 1024.0 eV in panel (c), as observed previously with Zn(II) in ZnO, [29] and Cd $3d$ electrons as a doublet at 406.1 eV and 407.9 eV, in good agreement with those of CdS. [30] Furthermore, based on the integrated peak areas, the ternary nanocomposites were found to consist of 57.6% of TiO_2 , 10.5% of ZnO and 31.9% of CdS.

The resulting nanocomposites exhibited consistent optical absorption characteristics. Figure 4 depicts the UV-vis diffuse reflectance spectra of the unmodified TiO_2 NTs and the related hybrids with ZnO and CdS. For the unmodified TiO_2 NTs (black curve), the absorption threshold can be identified at ca. 385 nm, consistent with the intrinsic band gap of ca. 3.2 eV for anatase TiO_2 . [31,32] Upon the deposition of a ZnO layer the absorption edge red-shifted to 420 nm (red curve); in comparison, the absorption edges for the

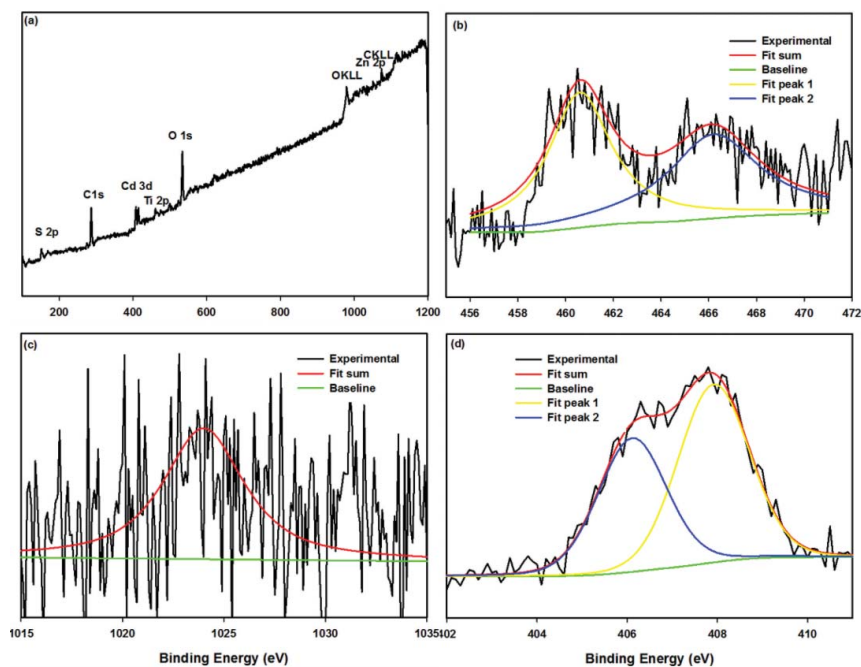


Figure 3. (a) XPS survey spectrum of $\text{TiO}_2/\text{ZnO}/\text{CdS}$ nanocomposites and high-resolution scans of the binding energies of (b) $\text{Ti } 2p$, (c) $\text{Zn } 2p$ and (d) $\text{Cd } 3d$ electrons in the $\text{TiO}_2/\text{ZnO}/\text{CdS}$ nanocomposites. Black lines are the experimental raw data and color lines are the deconvolution fitting.

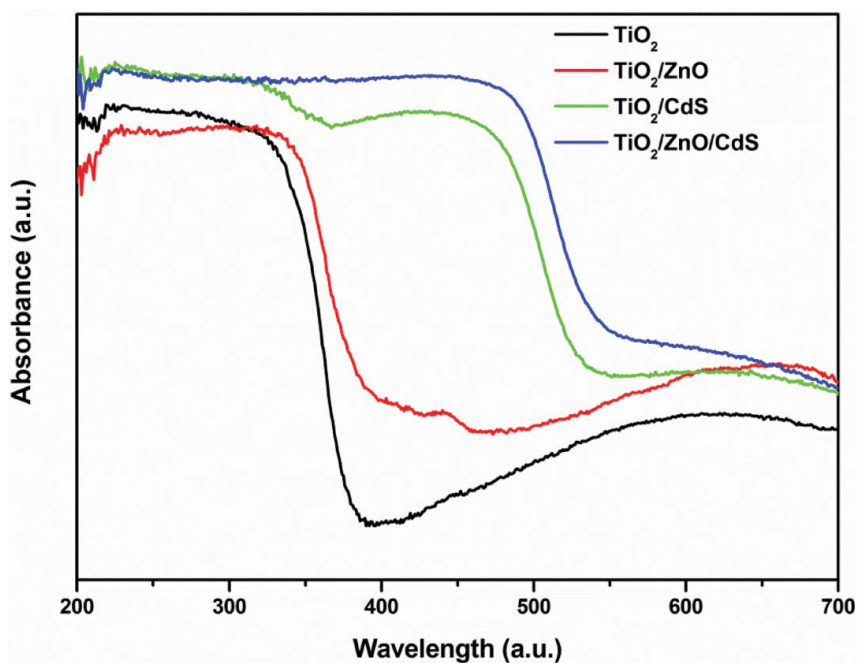


Figure 4. UV-vis diffuse reflectance spectra of unmodified TiO_2 nanotubes (black curve), TiO_2/CdS (green curve), TiO_2/ZnO (red curve) and $\text{TiO}_2/\text{ZnO}/\text{CdS}$ (blue curve) nanocomposites.

binary composites of TiO_2/CdS (green curve) and ternary hybrids of TiO_2 NTs/ ZnO/CdS (blue curve) red-shifted even further into the visible region at 550 nm and 575 nm, respectively.

The photocatalytic activities of these semiconductor composites were then evaluated by using the photodegradation of ARS as an illustrating example. Figure 5 shows the representative absorption spectra of an ARS solution under UV photoirradiation for different periods of time in the presence of a $\text{TiO}_2/\text{ZnO}/\text{CdS}$ nanocomposite. It can be seen that the characteristic absorption peak of ARS at 519 nm exhibited a remarkable decrease with increasing photoirradiation time, signifying the apparent activity of the nanocomposite in the degradation of ARS. Based on this, the fraction of ARS that was degraded can be determined at different photoirradiation times, as was depicted in Figure 6 (black curve). The catalytic activity of other catalysts was evaluated in a similar fashion and their reaction dynamics were also included in the figure for comparison.

Figure 6 depicts the reaction dynamics of ARS photodegradation in the presence of various TiO_2 -based catalysts. The fraction of ARS (c_t/c_0 , with c_0 being the starting ARS concentration at $t = 0$ min) that was removed was calculated by the diminishment of the ARS absorption peak at 519 nm (Figure 5). It can be seen that the efficiency of photocatalytic degradation of ARS increased in the order of $\text{TiO}_2 < \text{TiO}_2/\text{ZnO} < \text{TiO}_2/\text{CdS} < \text{TiO}_2/\text{ZnO}/\text{CdS}$. For instance, after 180 min of UV photoirradiation, the fraction of ARS that was degraded increased in the order of 39.2% (TiO_2) < 47.8% (TiO_2/ZnO) < 57.9%

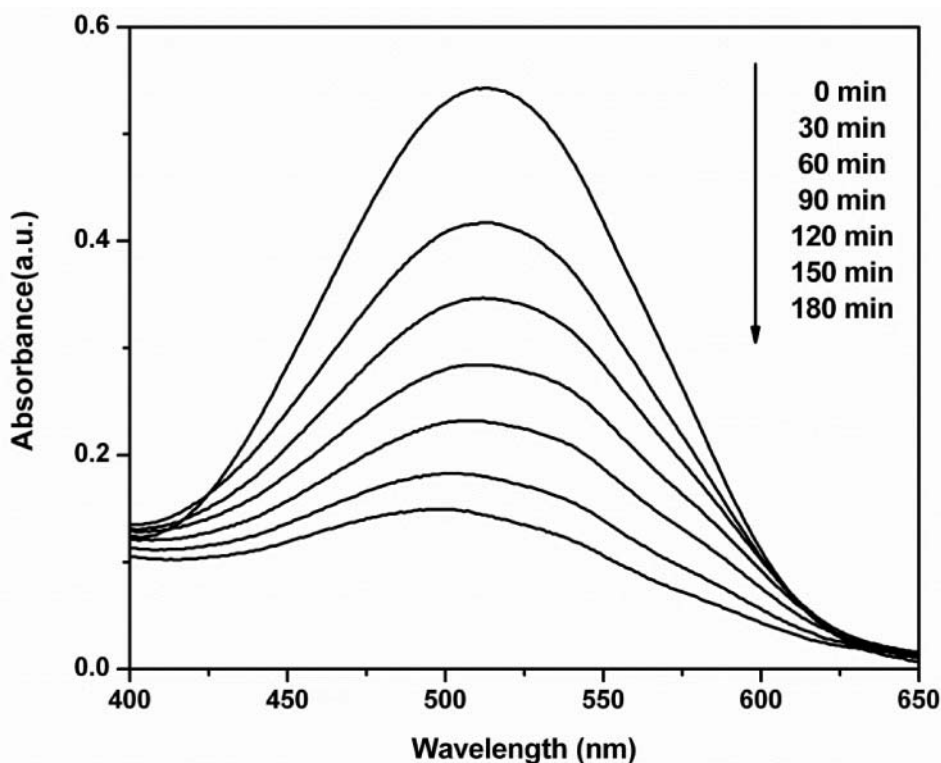


Figure 5. UV-vis absorption spectra of an ARS solution photodegraded by $\text{TiO}_2/\text{ZnO}/\text{CdS}$ ternary nanocomposites under UV photoirradiation for up to 180 min under magnetic stirring. ARS concentration is 40 mg mL^{-1} .

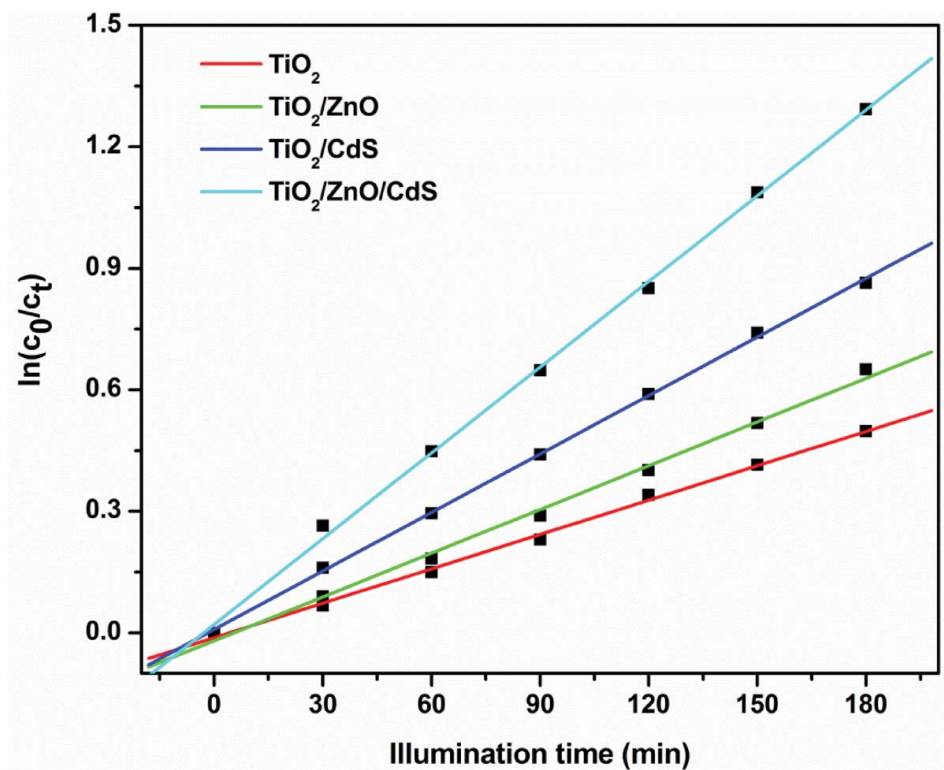


Figure 6. Comparison of photocatalytic degradation rates of TiO₂ nanotubes and the corresponding nanocomposites.

(TiO₂/CdS) < 75.0% (TiO₂/ZnO/CdS). Furthermore, the ARS concentration exhibited a linear profile in the semilog plot of $\ln(c_0/c_t)$ vs. illumination time (t), indicative of a first-order reaction. From the slope, the reaction rate constants (κ) can be estimated. One can see that for unmodified TiO₂ $\kappa = 0.17 \text{ h}^{-1}$, which increased to 0.22 h^{-1} for TiO₂/ZnO and to 0.29 h^{-1} for TiO₂/CdS and for ternary TiO₂/ZnO/CdS hybrids, κ was over two times greater at 0.44 h^{-1} . That is, the formation of a hybrid structure led to more than two times improvement of the photocatalytic performance.

The stability of the TiO₂/ZnO/CdS nanocomposites catalysts was then tested by repeat degradation of ARS for six times. After each use, the catalysts were washed and recycled. Figure 7 shows the removal rates of ARS by the same catalyst after 180 min of UV photoirradiation in six repeated tests, which were 75.0%, 72.56%, 70.44%, 68.52%, 64.78% and 62.79%, respectively. The small diminishment indicates good stability and performance of the ternary catalysts in ARS photodegradation.

These results may be accounted for by the formation of a cascade of energy structures within the ternary hybrids. Such a mechanism is schematically depicted in Figure 8. Specifically, as the conduction band (CB) of ZnO is ca. 0.02 V more negative than that of TiO₂ and 0.21 V more positive than that of CdS,[33] electrons are excited under UV irradiation from the valence bands (VBs) of TiO₂, ZnO and CdS to their respective CBs. As the CB decreases in energy in the order of TiO₂ < ZnO < CdS forming a stepwise band gap structure (Figure 8), the photogenerated electrons would most likely accumulate in

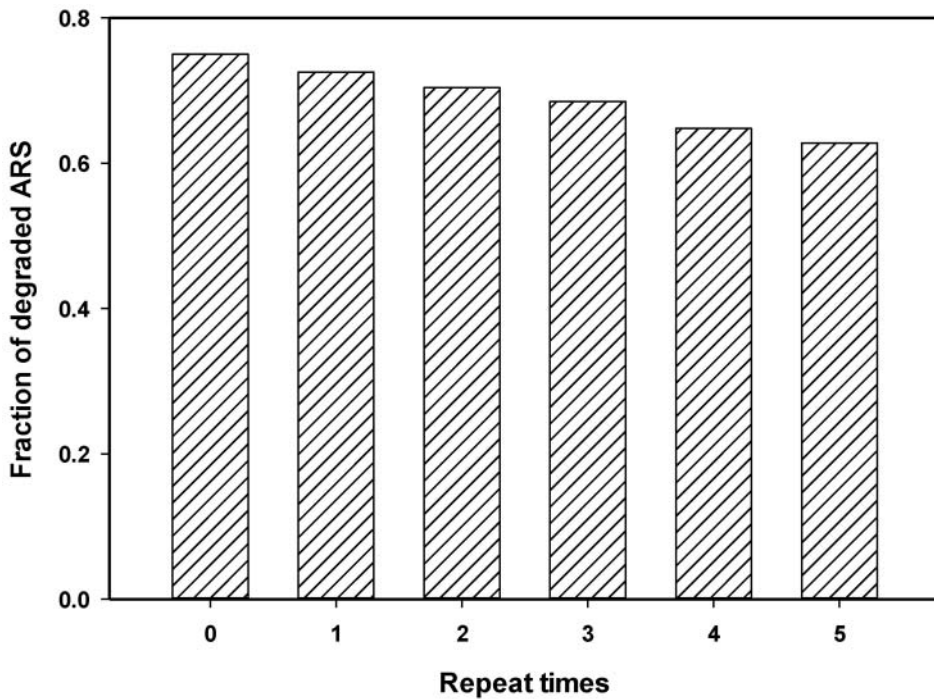


Figure 7. ARS removal rates in the presence of $\text{TiO}_2/\text{ZnO}/\text{CdS}$ nanocomposites catalysts in six repeated tests. In all measurements the UV photoirradiation time was 180 min. Other conditions were the same as those in Figure 6.

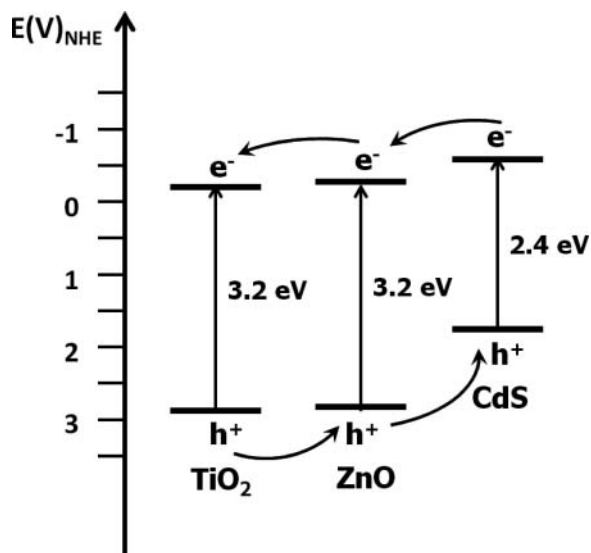


Figure 8. Energy diagram of TiO_2 NTs/ ZnO/CdS nanocomposites.

the CB of TiO₂; meanwhile the photogenerated holes moved to the VB of CdS, leading to effective charge separation. In this reaction mechanism, the photogenerated electrons in the TiO₂ CB would then participate in the reduction of dissolved oxygen (O₂) into superoxide (HOO[•]) or hydroxyl radicals (OH[•])[34]; meanwhile the photogenerated holes likely oxidize H₂O to form OH[•]. [22] Both of these OH[•] radicals then effectively oxidize ARS into mineral end products.[35]

4. Conclusion

A ternary hybrid based on TiO₂ NTs was prepared by the sequential deposition of a ZnO and CdS layer onto the NT surface. The photocatalytic activity of the resulting functional nanocomposite was examined by using the UV photodegradation of ARS as an illustrating example. The results showed that the ternary hybrids exhibited an activity that was more than two times that of the unmodified TiO₂ and also markedly better than those of the binary hybrids of TiO₂ with ZnO or CdS. The improved photocatalytic activity was ascribed to the formation of a cascade of electronic energy structures within the nanocomposites that facilitated interfacial charge separation and impeded charge recombination. The results highlight the fundamental significance of surface engineering in the manipulation and enhancement of the performance of titania-based photocatalysts.

Acknowledgements

C. Lin acknowledges the China Scholarship Council for a research fellowship. This work was supported, in part, by the National Natural Science Foundation of China (NSFC-50672089), the Program for New Century Excellent Talents in University (NCET-08-0511) and the Shandong Province Research Grants for MidCareer/Young Scientists (BS2010CL049). Work at UCSC was supported by the National Science Foundation (CBET-1258839, CHE-1012258 and CHE-1265635) and the Molecular Foundry, Lawrence Berkeley National Laboratory.

References

- [1] Hou Y, Li X, Zhao Q, Quan X, Chen G. Electrochemically assisted photocatalytic degradation of 4-chlorophenol by ZnFe₂O₄-modified TiO₂ nanotube array electrode under visible light irradiation. *Environ Sci Technol.* 2010;44:5098–5103.
- [2] Wang X, Zhao H, Quan X, Zhao Y, Chen S. Visible light photoelectrocatalysis with salicylic acid-modified TiO₂ nanotube array electrode for p-nitrophenol degradation. *J Hazard Mater.* 2009;166:547–552.
- [3] Lai Y, Zhuang H, Sun L, Chen Z, Lin C. Self-organized TiO₂ nanotubes in mixed organic–inorganic electrolytes and their photoelectrochemical performance. *Electrochim Acta.* 2009;54:6536–6542.
- [4] Zhai T, Xie S, Zhao Y, Sun X, Lu X, Yu M, Xu M, Xiao F, Tong Y. Controllable synthesis of hierarchical ZnO nanodisks for highly photocatalytic activity. *CrystEngComm.* 2012;14:1850–1855.
- [5] Zhang L, Tang X, Lu Z, Wang Z, Li L, Xiao Y. Facile synthesis and photocatalytic activity of hierarchical WO₃ core–shell microspheres. *Appl Surf Sci.* 2011;258:1719–1724.
- [6] Zhang N, Liu S, Xu Y-J. Recent progress on metal core@semiconductor shell nanocomposites as a promising type of photocatalyst. *Nanoscale.* 2012;4:2227–2238.
- [7] Zlamal M, Macak J, Schmuki P, Krysia J. Electrochemically assisted photocatalysis on self-organized TiO₂ nanotubes. *Electrochem Commun.* 2007;9:2822–2826.
- [8] Yoshida H, Lu Y, Nakayama H, Hirohashi M. Fabrication of TiO₂ film by mechanical coating technique and its photocatalytic activity. *J Alloys Compd.* 2009;475:383–386.

- [9] Liu Z, Zhang X, Nishimoto S, Jin M, Tryk DA, Murakami T, Fujishima A. Highly ordered TiO₂ nanotube arrays with controllable length for photoelectrocatalytic degradation of phenol. *J Phys Chem C*. 2008;112:253–259.
- [10] Zou T, Xie C, Liu Y, Zhang S, Zou Z, Zhang S. Full mineralization of toluene by photocatalytic degradation with porous TiO₂/SiC nanocomposite film. *J Alloys Compd*. 2013;552:504–510.
- [11] Zhao L, Jiang Q, Lian J. Visible-light photocatalytic activity of nitrogen-doped TiO₂ thin film prepared by pulsed laser deposition. *Appl Surf Sci*. 2008;254:4620–4625.
- [12] Zhao L, Chen X, Wang X, Zhang Y, Wei W, Sun Y, Antonietti M, Titirici M-M. One-step solvothermal synthesis of a carbon@TiO₂ dyade structure effectively promoting visible-light photocatalysis. *Adv Mater*. 2010;22:3317–3321.
- [13] Zhao H, Chen Y, Quan X, Ruan X. Preparation of Zn-doped TiO₂ nanotubes electrode and its application in pentachlorophenol photoelectrocatalytic degradation. *Chin Sci Bull*. 2007;52:1456–1461.
- [14] Le TT, Akhtar MS, Park DM, Lee JC, Yang OB. Water splitting on Rhodamine-B dye sensitized Co-doped TiO₂ catalyst under visible light. *Appl Catal B: Environ*. 2012;111–112:397–401.
- [15] Meng HL, Cui C, Shen HL, Liang DY, Xue YZ, Li PG, Tang WH. Synthesis and photocatalytic activity of TiO₂@CdS and CdS@TiO₂ double-shelled hollow spheres. *J Alloys Compd*. 2012;527:30–35.
- [16] Dai G, Yu J, Liu G. Synthesis and enhanced visible-light photoelectrocatalytic activity of p–n junction BiOI/TiO₂ nanotube arrays. *J Phys Chem C*. 2011;115:7339–7346.
- [17] Xu Z, Yu J. Visible-light-induced photoelectrochemical behaviors of Fe-modified TiO₂ nanotube arrays. *Nanoscale*. 2011;3:3138–3144.
- [18] Kim H-I, Kim J, Kim W, Choi W. Enhanced photocatalytic and photoelectrochemical activity in the ternary hybrid of CdS/TiO₂/WO₃ through the cascaded electron transfer. *J Phys Chem C*. 2011;115:9797–9805.
- [19] Bai J, Li J, Liu Y, Zhou B, Cai W. A new glass substrate photoelectrocatalytic electrode for efficient visible-light hydrogen production: CdS sensitized TiO₂ nanotube arrays. *Appl Catal B: Environ*. 2010;95:408–413.
- [20] Janitabar-Darzi S, Mahjoub AR. Investigation of phase transformations and photocatalytic properties of sol–gel prepared nanostructured ZnO/TiO₂ composites. *J Alloys Compd*. 2009;486:805–808.
- [21] Lin C-J, Lu Y-T, Hsieh C-H, Chien S-H. Surface modification of highly ordered TiO₂ nanotube arrays for efficient photoelectrocatalytic water splitting. *Appl Phys Lett*. 2009;94:113102.
- [22] Chen C, Xie Y, Ali G, Yoo SH, Cho SO. Improved conversion efficiency of CdS quantum dots-sensitized TiO₂ nanotube array using ZnO energy barrier layer. *Nanotechnology*. 2011;22:015202.
- [23] Li H, Cao L, Liu W, Su G, Dong B. Synthesis and investigation of TiO₂ nanotube arrays prepared by anodization and their photocatalytic activity. *Ceram Int*. 2012;38:5791–5797.
- [24] Kang XW, Chen SW. Photocatalytic reduction of methylene blue by TiO₂ nanotube arrays: effects of TiO₂ crystalline phase. *J Mater Sci*. 2010;45:2696–2702.
- [25] Roh S-J, Mane RS, Min S-K, Lee W-J, Lokhande CD, Han S-H. Achievement of 4.51% conversion efficiency using ZnO recombination barrier layer in TiO₂ based dye-sensitized solar cells. *Appl Phys Lett*. 2006;89:253512.
- [26] Oladejia IO, Chowa L, Liub JR, Chub WK, Bustamantec ANP, Fredricksena C, Schulte AF. Comparative study of CdS thin films deposited by single, continuous, and multiple dip chemical processes. *Thin Solid Films*. 2000;359:154–159.
- [27] Du B, Gao L, Lian X, Jiao Y. The synthesis and characterization of core-shell quantum dots via three-phase system. *J Chem Pharm Res*. 2012;4:2712–2719.
- [28] Siebert M, Albrecht K, Spiertz R, Keul H, Möller M. Reactive amphiphilic block copolymers for the preparation of hybrid organic/inorganic materials with covalent interactions. *Soft Matter*. 2011;7:587–594.
- [29] Seong JW, Kim KH, Beag YW, Koh SK, Yoon KH. Effect of low substrate deposition temperature on the optical and electrical properties of Al₂O₃ doped ZnO films fabricated by ion beam sputter deposition. *J Vac Sci Technol A*. 2004;22:1139–1145.
- [30] Islam AKMM, Mukherjee M. Application of differential charging in XPS for structural study of Langmuir–Blodgett films. *J Phys Condens Matter*. 2011;23:435005.

- [31] Pelaez M, Nolan NT, Pillai SC, Seery MK, Falaras P, Kontos AG, Dunlop PSM, Hamilton JWI, Byrne JA, O'Shea K, Entezari MH, Dionysiou DD. A review on the visible light active titanium dioxide photocatalysts for environmental applications. *Appl Catal B: Environ.* 2012;125:331–349.
- [32] Carey MJ, Burlakov VM, Henry BM, Kirov KR, Webster GR, Assender HE, Briggs GAD, Burn PL, Grovenor CRM. Nanocomposite titanium dioxide/polymer photovoltaic cells: effects of TiO₂ microstructure, time and illumination power. *Proc SPIE: Org Photovolt IV.* 2004;5215:32–40.
- [33] Xu Y, Schoonen MAA. The absolute energy positions of conduction and valence bands of selected semiconducting minerals. *Am Mineral.* 2000;85:543–556.
- [34] Lin CJ, Yu YH, Liou YH. Free-standing TiO₂ nanotube array films sensitized with CdS as highly active solar light-driven photocatalysts. *Appl Catal B: Environ.* 2009;93:119–125.
- [35] Liu G, Li X, Zhao J, Horikoshi S, Hidaka H. Photooxidation mechanism of dye alizarin red in TiO₂ dispersions under visible illumination: an experimental and theoretical examination. *J Mol Catal A: Chem.* 1999;153:221–229.